Cancer Research

Multinucleation and Mesenchymal-to-Epithelial Transition Alleviate Resistance to Combined Cabazitaxel and Antiandrogen Therapy in Advanced Prostate Cancer

Sarah K. Martin[1], Hong Pu[2], Justin C. Penticuff[2], Zheng Cao[2], Craig Horbinski[1,3,4], and Natasha Kyprianou[1,2,3,4,5]

Abstract

Patients with metastatic castration-resistant prostate cancer (CRPC) frequently develop therapeutic resistance to taxane chemotherapy and antiandrogens. Cabazitaxel is a second-line taxane chemotherapeutic agent that provides additional survival benefits to patients with advanced disease. In this study, we sought to identify the mechanism of action of combined cabazitaxel and androgen receptor (AR) targeting in preclinical models of advanced prostate cancer. We found that cabazitaxel induced mitotic spindle collapse and multinucleation by targeting the microtubule depolymerizing kinesins and inhibiting AR. In androgen-responsive tumors, treatment with the AR inhibitor, enzalutamide, overcame resistance to cabazitaxel. Combination treatment of human CRPC xenografts with cabazitaxel and enzalutamide reversed epithelial–mesenchymal transition (EMT) to mesenchymal–epithelial transition (MET) and led to multinucleation, while retaining nuclear AR. In a transgenic mouse model of androgen-responsive prostate cancer, cabazitaxel treatment induced MET, glandular redifferentiation, and AR nuclear localization that was inhibited by androgen deprivation. Collectively, our preclinical studies demonstrate that prostate tumor resistance to cabazitaxel can be overcome by antiandrogen-mediated EMT-MET cycling in androgen-sensitive tumors but not in CRPC. Moreover, AR splice variants may preclude patients with advanced disease from responding to cabazitaxel chemotherapy and antiandrogen combination therapy. This evidence enables a significant insight into therapeutic cross-resistance to taxane chemotherapy and androgen deprivation therapy in advanced prostate cancer. *Cancer Res; 76(4); 912–26. ©2015 AACR.*

Introduction

Androgen deprivation therapy (ADT) has been used as a standard treatment for patients with advanced prostate cancer since the historic discovery by Charles Huggins 65 years ago (1). All patients, however, ultimately develop castration-resistant prostate cancer (CRPC) with recurrence to lethal disease. Progression to metastatic CRPC (mCRPC) is characterized by aberrant expression of the androgen receptor (AR), *de novo* intraprostatic androgen production, and cross-talk between androgen signaling with other oncogenic pathways (2, 3). Recent antiandrogen therapies, such as abiraterone acetate and enzalutamide, although effectively target the androgen signaling axis (4–6), due to the addiction of CRPC cells to ARsignaling and constitutively active AR splice variants, resistance develops and disease recurs (7–9). Taxanes (docetaxel and cabazitaxel) are the mainstay of chemotherapy for metastatic CRPC patients who developed resistance to antiandrogen therapy. First-generation taxanes, like docetaxel (Taxotere), target the cytoskeleton by stabilizing the interaction of β-tubulin subunits of microtubules preventing depolymerization, inducing G_2–M arrest and apoptosis (10). Unliganded AR is sequestered in the cytoplasm by the HSP90 supercomplex and upon binding to the ligand, DHT, dimerizes and translocates to the nucleus (11, 12). Nuclear AR binds androgen-responsive elements of DNA and transcriptionally activates genes promoting prostate cell growth (11). Taxanes bind to β-tubulin subunits of microtubules, stabilizing their interaction and preventing depolymerization of the microtubule structure and leading to apoptosis (13, 14). Work by our group and others established that docetaxel chemotherapy inhibits AR trafficking and nuclear translocation, thus preventing its transcriptional activity (15–17). Taxanes also upregulate forkhead box 01 (FOXO1), a transcriptional repressor of AR, resulting in the inhibition of ligand-dependent and -independent transcription and downregulation of AR and prostate-specific antigen (PSA) expression (18, 19).

The therapeutic impact of taxanes in mCRPC and improving patient survival has been attributed to microtubule stabilization and AR-targeting ADT (18, 20). Despite an initial efficacy and a survival advantage in patients with mCRPC, resistance to taxane chemotherapy invariably develops, leading to disease progression (21). Mechanisms implicated in the development of docetaxel resistance include high affinity of the drug for the P-glycoprotein

[1]Department of Molecular and Cellular Biochemistry, University of Kentucky College of Medicine, Lexington, Kentucky. [2]Department of Urology, University of Kentucky, Lexington, Kentucky. [3]Department of Pathology and Laboratory Medicine, Lexington, Kentucky. [4]Markey Cancer Center, University of Kentucky, Lexington, Kentucky. [5]Department of Toxicology and Cancer Biology, University of Kentucky, Lexington, Kentucky.

Note: Supplementary data for this article are available at Cancer Research Online (http://cancerres.aacrjournals.org/).

Corresponding Author: Natasha Kyprianou, University of Kentucky College of Medicine, 800 Rose Street, 306 Combs Building, Lexington, KY 40536. Phone: 859-323-9812; Fax: 859-257-9608; E-mail: nkypr2@email.uky.edu

doi: 10.1158/0008-5472.CAN-15-2078

drug efflux pump, mutational alterations in tubulin, and epithelial– mesenchymal transition (EMT; refs. 20–22). The FDA has recently approved several promising agents including Jevtana (cabazitaxel, Xtandi (enzalutamide, MDV3100), and Provenge (sipleucel-T) providing additional survival benefits to patients with advanced disease (23, 24). Cabazitaxel is the second-line taxane chemotherapy, with significantly decreased affinity for the P-glycoprotein pump for increased cellular retention (14). The nonsteroidal, antiandrogen enzalutamide (MDV3100) was rationally designed from the AR crystal structure (4, 24, 25). Functionally, MDV blocks androgen signaling by preventing binding of AR to DHT, blocking AR translocation into the nucleus, and inhibiting AR from binding to androgen-responsive elements on DNA (12, 26). Recent clinical evidence suggests that the AR splice variant V7 confers therapeutic resistance to enzalutamide in CRPC patients (8, 9, 27).

The process of EMT, featuring characteristic phenotypic manifestations and driven by molecular programming, confers invasive, metastatic, and stem cell–like properties in epithelial-derived tumors with acquired resistance to apoptosis (28–32). In this study, we investigated the contribution of EMT to resistance to cabazitaxel and antiandrogens in preclinical models of advanced prostate cancer. Our findings indicate for the first time that cabazitaxel induces multinucleation by targeting kinesin expression and reverses EMT to mesenchymal–epithelial transition (MET) *in vitro* and *in vivo*. Cabazitaxel also sustains nuclear AR, conferring resistance that can be overcome by antiandrogens in androgen-responsive tumors. In CRPC models harboring a cohort of AR variants, combination treatment of cabazitaxel with antiandrogen promoted epithelial redifferentiation by activating MET.

Materials and Methods

Cell lines and transfections

Human prostate cancer cell lines, the androgen-independent cell lines PC3 and DU145, the CRPC cancer cell line 22Rv1, and the androgen-sensitive human prostate cancer cell lines LNCaP and VCaP were obtained from ATCC. Cell lines were obtained every year between 2010 and 2014 and have been authenticated and tested for mycoplasma in September 2011, June 2012, and November 2013 by Q11 short tandem repeat (STR; method of Masters and colleagues 2012: Authentication of human cell lines: standardization of STR profiling; DDC Medical). PC3 AR variant transfectants PC3v7, PCv12, and PC3v567es were generated in this laboratory using plasmids provided by Drs. S. Plymate (University of Washington, Seattle, WA) and J. Luo (Johns Hopkins Brady Urological Institute, Baltimore, MD). TGFβ-responsive LNCaPTβRII were generated and characterized in this laboratory (33, 34). All cell lines, but VCaP cells, were maintained in RPMI1640 (Invitrogen) and 10% FBS, 100 U/mL penicillin and 100 μg/mL streptomycin in a 5% CO_2 incubator (37°C). The VCaP cells were cultured in DMEM (ATCC). Cells were seeded in 10% CSS and stimulated by DHT (Sigma-Aldrich) or R1881 (1 nmol/L).

Drugs

Cabazitaxel (Jevtana) was generously provided by Sanofi Aventis. For the *in vivo* administration, cabazitaxel was prepared by mixing ethanol, polysorbate 80, and 5% (w/v) glucose in sterile water (1:1:18). Solutions were administered intravenously as a slow bolus. Cabazitaxel stock (500 μmol/L) was prepared in 100% ethanol and stored at −20°C. MDV3100 was purchased from Selleck Chemicals. For *in vivo* administration in mice, MDV3100 was prepared in DMSO, diluted with sterile PBS (75% PBS and 25% cabazitaxel–DMSO solution), and injected intraperitoneally.

Antibodies

The antibody against the AR (N-20) protein was purchased from Santa Cruz Biotechnology. Antibodies against tubulin, N-cadherin, mitotic centromere–associated kinesin (MCAK; KIF2C), HSET, CD31, and phospho-histone H3 (pH3) were obtained from Abcam Cell Signaling; antibodies against cleaved caspase-3, GAPDH, E-cadherin, and cytokeratin-18 proteins were obtained from Cell Signaling Technology. The ZEB1 antibody was obtained from Bethyl Laboratories.

Western blot analysis

Total cellular protein was extracted from cell lysates by homogenization with RIPA buffer (Cell Signaling Technology); subcellular fractionation was performed using NE-PER nuclear-cytoplasmic fraction kit (Thermo Scientific). Protein samples were loaded into 4% to 15% SDS–polyacrylamide gels (Bio-Rad) and subjected to electrophoretic analysis and blotting. Membranes were subsequently incubated with the Amersham ECL Plus Western Blotting Detection System (Amersham, GE Healthcare) and auto-radiographed using X-ray film (Denville Scientific). Protein expression bands were normalized to GAPDH expression.

Cell viability assay

The effect of the various treatments on prostate cancer cell viability was evaluated using the Thiazolyl Blue Tetrazolium bromide (MTT) assay. Cells were seeded into 24-well plates and after grown to 60% to 75% confluence, were treated with vehicle control (VHC; DMSO, Sigma-Aldrich), cabazitaxel, MDV3100, and combination in RPMI1640 with 10% CSS for 24 hours (or DMEM for VCaP). At the termination of exposure, cells were aspirated and rinsed with PBS, then treated with 250 μL/well MTT (1 mg/mL) for 30 minutes at 37°C. Absorbance was measured at 570 nm using μQuant Spectrophotometer (Biotech Instruments Inc.).

Migration assays

Cells were seeded in 6-well plates, and at 65% to 70% density, the cell monolayers were wounded. After 24 hours, the number of migrating cells toward the center of the wound was counted in three different fields.

Quantitative RT-PCR analysis

***In vitro samples.*.** RNA was extracted with the TRIzol reagent (Life Technologies), and RNA samples (1 μg) were subjected to reverse transcription using the Reverse Transcription System (Promega). TaqMan real-time RT-PCR (Life Technologies) analysis of the cDNA samples was conducted in an ABI7700 Sequence Detection System (Applied Biosystems, Inc.) using the following specific primers: PSA (KLK3; Hs02576345_m1), AR (Hs00171172_m1), KIF2C (Hs00901710_m1), FOXO1 (Hs01054576_m1), KIFC1 (Hs00954801_m1), E-cadherin (CDH1; Hs01023894_m1), N-cadherin (CDH2; Hs00983056_m1), Twist (TWIST1; Hs01675818_s1), vimentin (VIM; Hs00185584_m1), and 18S

rRNA (4319413E; Applied Biosystems, Life Technologies). Data represent average values from three independent experiments; numerical data were normalized to 18s rRNA and expressed relative to controls.

Immunofluorescent confocal microscopy

Cells were plated (1×10^5) on cover glass in 6-well plates. After 24 to 48 hours, cells were exposed to medium (RPMI1640 with 10% CSS) in the presence of DHT (1 nmol/L), cabazitaxel (35–100 nmol/L), MDV3100 (1 μmol/L), or in combination of the two agents. Following treatment, cells were fixed in 100% methanol and permeabilized with 0.1% Triton X-100 in sterile PBS. Fixed cells were incubated overnight with primary antibody specific for AR (N-20) and tubulin (Abcam Cell Signaling) at 4°C with gentle rocking and the appropriate Alexa-Fluor (Life Technologies) fluorescent secondary (1.5 hours, room temperature). Slides were mounted using Vectashield mounting medium with DAPI and were visualized using a FV1000 Confocal Microscope (Markey Cancer Center Core, University of Kentucky, Lexington, KY).

Flow cytometric analysis

The human prostate cancer cells harboring the AR variants PC3v567es and 22Rv1 cells were exposed to various treatments (MDV, cabazitaxel, or combination for 24–96 hours) and subjected to washing with PBS in 0.1% BSA. Cells were subsequently fixed with 100% ethanol (−20°C). For cell-cycle analysis, cells were incubated with propidium iodide solution with RNase A (10 μg/mL) overnight at 4°C. Samples were analyzed using Becton-Dickinson FACSCalibur (flow cytometry core at the University of Kentucky, Lexington, KY).

In vivo tumor targeting studies

All animal experiments were performed in accordance with the guidelines approved by the Animal Care and Use Committee of the University of Kentucky and according to the NIH (Bethesda, MD) recommendations and reporting standards. Male nude mice (5–6-week-old) were subcutaneously injected with 22Rv1 cells (2×10^6 cells), and after tumors were palpable, mice were divided into four groups, 5 mice/group: (i) control group receiving 1% medium/0.1% Tween-20 daily via oral gavage; (ii) cabazitaxel treatment group mice received cabazitaxel (day 1 and 4, 5 mg/kg; day 8 and 14, 2.5 mg/kg) via tail-vein injection for 2 weeks; (c) enzalutamide group mice receiving 30 mg/kg MDV3100 via intraperitoneal injection for 2 weeks; (iv) and cabazitaxel and MDV3100 combination group mice receiving both cabazitaxel and enzalutamide for 2 weeks. Tumors were measured twice a week, and the volume was calculated (length × width × 0.5236). Prostate tumor xenografts were harvested at 4 days after the last treatment and histopathologically analyzed. Formalin-fixed paraffin-embedded sections were subjected to immunostaining for expression and localization of AR, mitotic kinesins, EMT, vascularity (CD31), and apoptosis (TUNEL, EMD Millipore). TUNEL analysis of apoptotic cells *in situ* was performed as previously described (35).

Transgenic mouse model of prostate cancer progression

Mice were maintained under environmentally controlled conditions and subjected to a 12-hour light/dark cycle with food and water *ad libitum*. Mice TRAMP+/DNTGFβRII+ (16–18 weeks; ref. 35) were matched with littermates and were treated with either VHC or highest nontoxic dose of cabazitaxel (day 0 and 3, 10 mg/kg; day 7 and 11, 5 mg/kg) dosed intraperitoneally and harvested on day 14. TRAMP+/DNTGFβRII+ male mice were castrated and treated with cabazitaxel (day 3 and 7, 10 mg/kg; day 11 and 15, 5 mg/kg) and harvested on day 18.

Immunohistochemical analysis

Tissue specimens from human CRPC (22Rv1) xenografts and transgenic mouse prostate tumors were formalin-fixed and paraffin-embedded; serial sections (5 μm) were subjected to immunohistochemical analysis using antibodies against E-cadherin, N-cadherin, AR (N-20), MCAK, HSET, pH3, ZEB1, cytokeratin-18, and CD31. After blocking nonspecific binding, sections were incubated with primary antibody (overnight, 4°C) and were subsequently exposed to biotinylated goat anti-rabbit IgG (2 hours, room temperature) and horseradish peroxidase–streptavidin (EMD Millipore). Signal/Color detection was achieved with SigmaFast 3, 3′-diaminobenzidine tablets (Sigma-Aldrich) and counterstained with hematoxylin. TUNEL analysis of apoptotic cells was performed as previously described (35). Images were captured via light microscopy (40× and 100×) using an Olympus BX51 microscope (Olympus America). The intensity and level of immunoreactivity was recorded by two independent observers.

Statistical analysis

Student *t* test, one-way, or two-way ANOVA were performed using GraphPad Prism 6 software to determine the statistical significance of difference between means/treatments. All numerical data are presented as mean ± SEM. Statistical significance was set at $P < 0.05$.

Results

Significance of AR status in prostate cancer cell response to cabazitaxel

The preclinical efficacy of cabazitaxel chemotherapy against prostate cancer was originally demonstrated using the androgen-independent human cancer cell line, DU145 (lacking AR) as a model (14). To establish the cellular response of androgen-sensitive and CRPC cancer cells to cabazitaxel treatment, a panel of human prostate cancer cell lines with varying AR expression status was used. A dose–response analysis of prostate cancer cell viability to increasing concentrations of cabazitaxel (10–500 nmol/L) for 96 hours demonstrated that DU145 cells were highly sensitive to cabazitaxel treatment consistent with earlier reports (14; Fig. 1A). A time-course analysis of the temporal response to increasing treatment periods to cabazitaxel (100 nmol/L) was also conducted (Fig. 1B). The androgen-independent PC3 cells exhibited a similar sensitivity to cabazitaxel as the DU145 cells (Fig. 1A and B). In contrast, PC3 cells with forced overexpression of the AR splice variant v567es (PC3v567es) were resistant to cabazitaxel even at very high doses of the drug, compared with parental PC3 cells (Fig. 1A). The CRPC cell line 22Rv1, harboring a mix of AR variants as well as the full-length AR, exhibited relative resistance to low doses of cabazitaxel and short treatment periods (24–48 hours), but after longer treatment (over 72 hours), there was a significant loss of cell viability (Fig. 1A and B). The androgen-responsive cells VCaP (full-length AR) were resistant to cabazitaxel (500 nmol/L) compared with LNCaP and LNCaPTβRII cells (Fig. 1A and B).

To examine the effect of AR-targeting inhibition by the anti-androgen (MDV3100, MDV) to sensitize prostate cancer cells to cabazitaxel, human prostate cancer cell lines were treated with

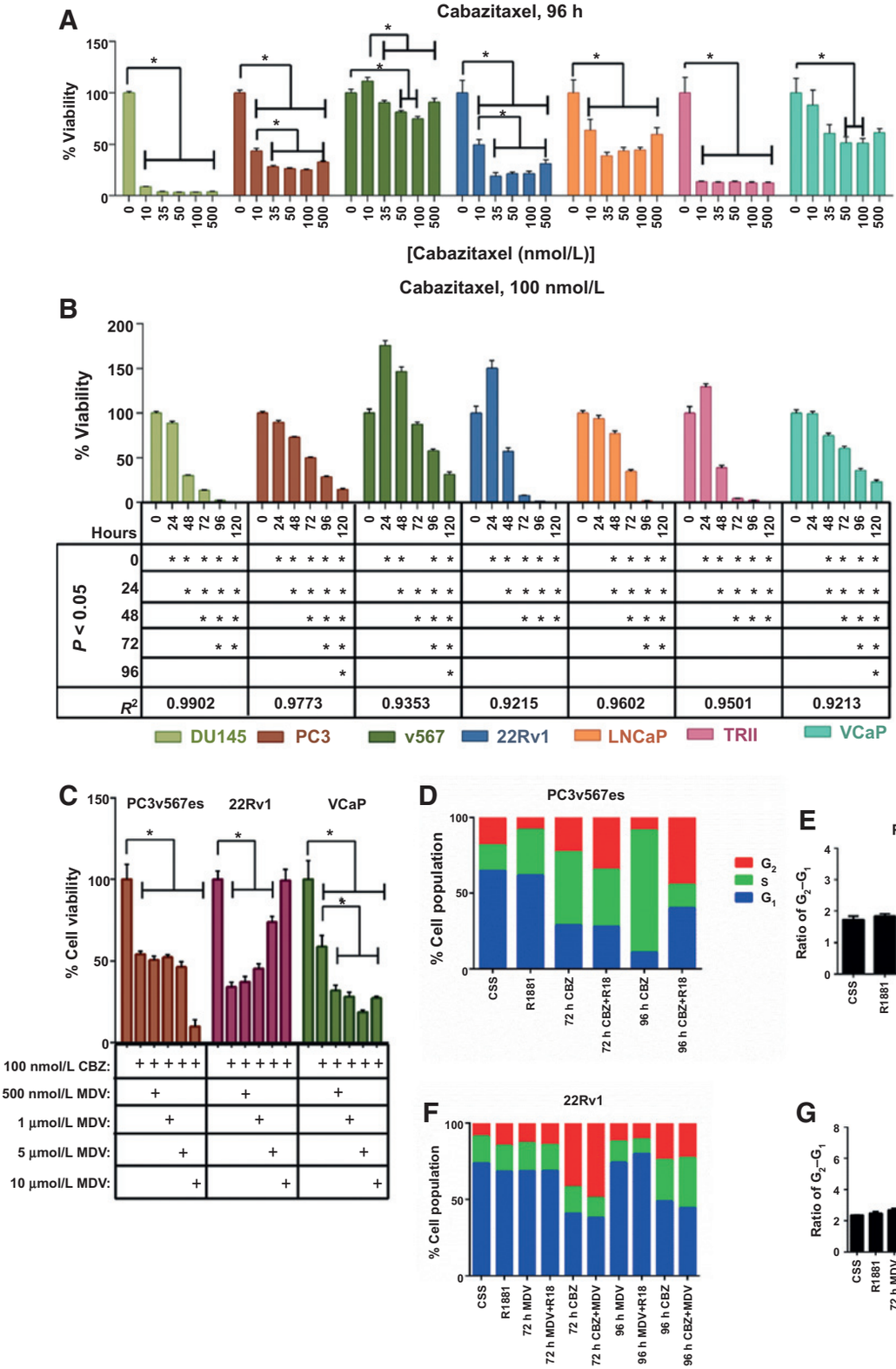

Figure 1.
Human prostate cancer cell response to cabazitaxel and AR targeting. A, dose–response analysis of human prostate cancer cells, DU-145, PC-3, PC3v567es, 22Rv1, LNCaP, LNCaPTβRII, and VCaP to cabazitaxel (10–500 nmol/L) for 96 hours. Cell viability was evaluated by the MTT assay. B, time course of cell viability response to cabazitaxel (100 nmol/L). C, effect of cabazitaxel alone or in combination with the antiandrogen (MDV, 1–10 μmol/L). D and E, cabazitaxel induces G_2 and S-phase arrest in PC3v567es cells. F and G, cell-cycle analysis of CRPC 22Rv1 cells in response to treatment. Data from three independent experiments ± SEM; *, $P < 0.05$ as determined by one-way ANOVA.

cabazitaxel alone (100 nmol/L) or in combination with MDV (1–10 μmol/L). The PC3v567es cells did not exhibit further cell death as a result of antiandrogen treatment compared with cabazitaxel alone (except at supraphysiologic concentrations; Fig. 1C). For the androgen-sensitive and cabazitaxel-resistant VCaP cells (Fig. 1A), exposure to increasing concentrations of MDV in combination with cabazitaxel resulted in a significant loss of viability ($P < 0.05$; Fig. 1C). The CRPC 22Rv1 cells (harboring a mixture of full-length AR and AR splice variants) exhibited loss of viability in response to cabazitaxel alone; however, combination of the taxane with MDV at high concentrations (10 μmol/L) led to an increase in cell viability compared with the single cabazitaxel treatment (Fig. 1C) and untreated control cells. Cell-cycle analysis revealed that for the PC3v567es cells, cabazitaxel treatment promotes G_2 and S-phase arrest (Fig. 1D and E). For CRPC 22Rv1 cells, exposure to cabazitaxel alone or in combination with enzalutamide (96 hours) resulted in a significant G_2 arrest (Fig. 1F and G). Treatment of PC3v567es and 22Rv1 cells with cabazitaxel led to increased prostate cell population in the S and G_2 phase regardless of androgens.

Recent work from this laboratory demonstrated that combination therapy of taxanes (docetaxel) and N-terminal targeting of AR with novel antiandrogens enhanced the therapeutic efficacy of taxane against CRPC tumor growth (36). Thus, we comparatively analyzed the dose response of prostate cancer cells to docetaxel (microtubule targeting) and MDV (AR targeting) given as single agents or in combination (Supplementary Fig. S1A–S1C). The PC3, PCv567es, 22Rv1, and LNCaP cells exhibited resistance to MDV, but all the cell lines showed partial sensitivity to docetaxel (Supplementary Fig. S1A and S1B, respectively). Combination of docetaxel and MDV led to a significant loss of cell viability for all of the prostate cancer cell lines (Supplementary Fig. S1C). Overexpression of AR variants in PC3 cells resulted in stable clones PC3567es, PC3v7, and PCv12 that all exhibited a significant increase in their migration potential compared with parental control cells (Supplementary Fig. S1D).

Effect of cabazitaxel on AR expression, localization, and activity

Docetaxel chemotherapy has been shown to impair prostate cancer growth by preventing the physical translocation of cytoplasmic AR into the nucleus ultimately inhibiting the activity of AR-regulated target genes (PSA; refs. 15–17). LNCaP and VCaP cells grown in CSS media were subjected to confocal microscopy analysis that indicated a diffused distribution of AR between the cytoplasm and the nucleus in LNCaP control cells (Fig. 2A). Treatment with DHT (Fig. 2A) resulted in AR translocation to the nucleus. Treatment with the antiandrogen MDV (1 μmol/L; 24 hours) increased cytoplasmic AR with no apparent effect on microtubule structural network (Fig. 2A; ref. 4). Cabazitaxel reduced overall AR immunoreactivity, while it sustained the nuclear localization of AR regardless of androgens or antiandrogens. Treatment of VCaP cells for 24 hours with MDV followed by pulsing with DHT (2 hours) was analyzed by confocal microscopy (Supplementary Fig. S2A). AR localization was primarily confined to the nucleus, indicating that MDV was unable to completely block the androgen-mediated AR nuclear translocation (Supplementary Fig. S2A). Treatment of VCaP with cabazitaxel (96 hours) leads to AR nuclear localization independently of androgens (Fig. 2A and Supplementary Fig. S2). There was a significant impact by cabazitaxel treatment on the microtubule structure, with tubule bundling on the periphery of the cell and complete loss of fibrous microtubule network appearance (Fig. 2A; green). The effects on the microtubule appearance were consistently detected in response to cabazitaxel, associated with remarkable multinucleation in both cell lines (zoom images; Fig. 2A and Supplementary Fig. S2A). The PC3v567es cells expressing AR variant v567es (resistant to cabazitaxel; Fig. 1A and B) were treated with cabazitaxel and subjected to confocal microscopy. Cabazitaxel exerts the bundling effect on microtubule structures (Supplementary Fig. S3), reduces AR levels, and fails to sustain nuclear localization of AR v567es. Extensive multinucleation is observed for PC3v567es cells in response to cabazitaxel.

To determine the effect of cabazitaxel treatment on AR expression, LNCaP and VCaP prostate cancer cells were treated for 24, 48, or 72 hours with cabazitaxel alone or pulsed with DHT for 3 hours prior to cell lysis and Western blot analysis. Cabazitaxel treatment for 72 hours markedly reduced AR protein levels in the androgen-sensitive prostate cancer cell lines, LNCaP and VCaP (Fig. 2B and Supplementary Fig. S2A, respectively). Expression of β-tubulin was not affected. Cabazitaxel treatment (48 hours) led to caspase-3 cleavage, indicating apoptosis induction (Fig. 2B). To confirm the effect of cabazitaxel on AR localization, we performed subcellular fractionation analysis in LNCaP cells after exposure to cabazitaxel (24, 48, or 72 hours) alone or pulsed with R1881 (1 nmol/L for 2 hours). Androgens predictably increased nuclear AR expression compared with controls (Fig. 2C). Cabazitaxel treatment for 24 to 48 hours decreased AR levels in LNCaP cells, while there was nuclear retention of AR (Fig. 2C); by 72 hours, AR levels were diminished in both cytosolic and nuclear fractions (Fig. 2C). To establish that the effect of cabazitaxel on AR expression was a consequence of transcriptional inhibition, the AR mRNA levels were evaluated. LNCaP cells were treated with cabazitaxel (24, 48, or 72 hours) alone or pulsed with DHT for 2 hours prior to mRNA extraction. Cabazitaxel treatment (24 hours) led to downregulation of AR mRNA (Fig. 2D). Moreover, cabazitaxel significantly inhibited expression of the AR-regulated gene PSA and AR interactor FOXO1 (Fig. 2E and F), respectively, indicating targeting of AR transcriptional activity by cabazitaxel. A similar effect of cabazitaxel on AR-regulated gene expression was also found for the VCaP cells (Supplementary Fig. S2C–S2E).

Cabazitaxel causes multinucleation in prostate cancer cells by targeting kinesins

As chemotherapeutic agents, taxanes can effectively target the microtubules and the mitotic spindle apparatus, thus blocking cellular division by inducing G_2–M arrest and apoptosis (37). Confocal microscopy analysis revealed that three human prostate cancer cell lines with different AR status, DU145 cells (AR-negative), PC3v7 AR variant, LNCaP (mutant AR), and VCaP (full-length AR) cells exhibited increased incidence of multinucleation in response to cabazitaxel treatment (Fig. 3A). In the LNCaP cells, there was a disruption of the mitotic spindle and monoastral spindle formation. Overexpression of promitotic kinesins can facilitate taxane resistance due to their microtubule depolymerizing action. Targeting of kinesins by cabazitaxel was profiled by analyzing the expression of a subset of mitotic kinesins in human prostate cancer cell lines (Fig. 3B). MCAK kinesin plays an important role in facilitating spindle pole capture and also acts as a microtubule depolymerizing factor. HSET functionally mediates cytokinesis. LNCaP cells express relatively low kinesin levels, whereas VCaP cells exhibit

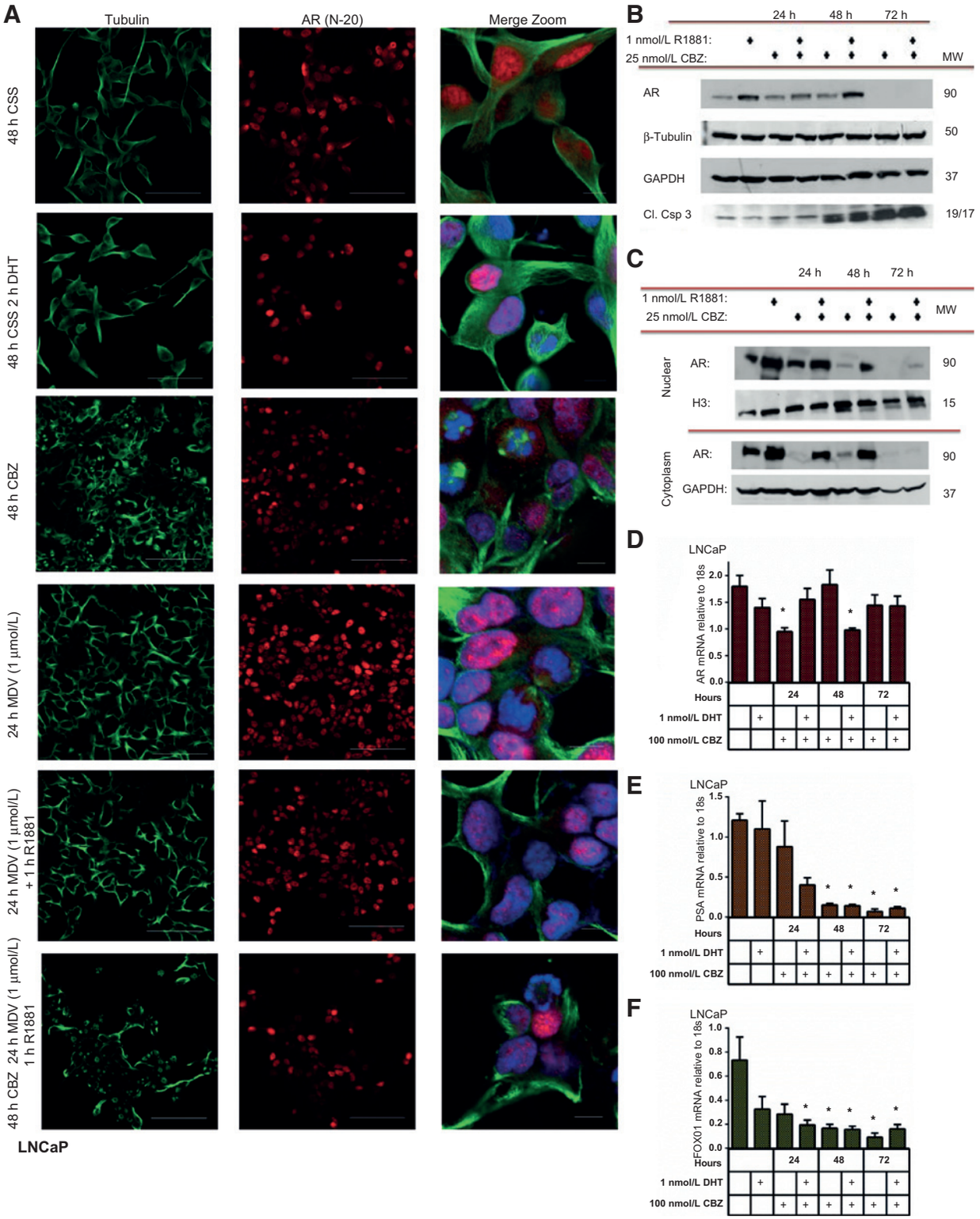

Figure 2.
Effect of cabazitaxel on AR localization and expression in prostate cancer cells. A, representative confocal images of AR expression in LNCaP cells. Cells were treated with MDV3100 (1 μmol/L, 24 hours) and cabazitaxel (25 nmol/L, 96 hours; in the presence or absence of DHT), as single agents or in combination, and subjected to fluorescent labeling for tubulin, AR (N-20) and DAPI (nucleus). Magnification, ×40. Scale bars, 100 μm. B, effect of cabazitaxel on AR (N-20), β-tubulin, and cleaved caspase-3 (Cl. Csp-3) protein levels in LNCaP cells. GAPDH was used as a loading control. C, subcellular fractionation of LNCaP after treatment with cabazitaxel. Immunoblot of AR (N-20), histone H3, and GAPDH protein expression. D–F, RT-PCR analysis shows cabazitaxel-induced downregulation of AR, PSA, and FOXO1 gene expression. Data represent mean of three independent experiments in duplicate ± SEM; *, $P < 0.05$ as determined by a two-way ANOVA.

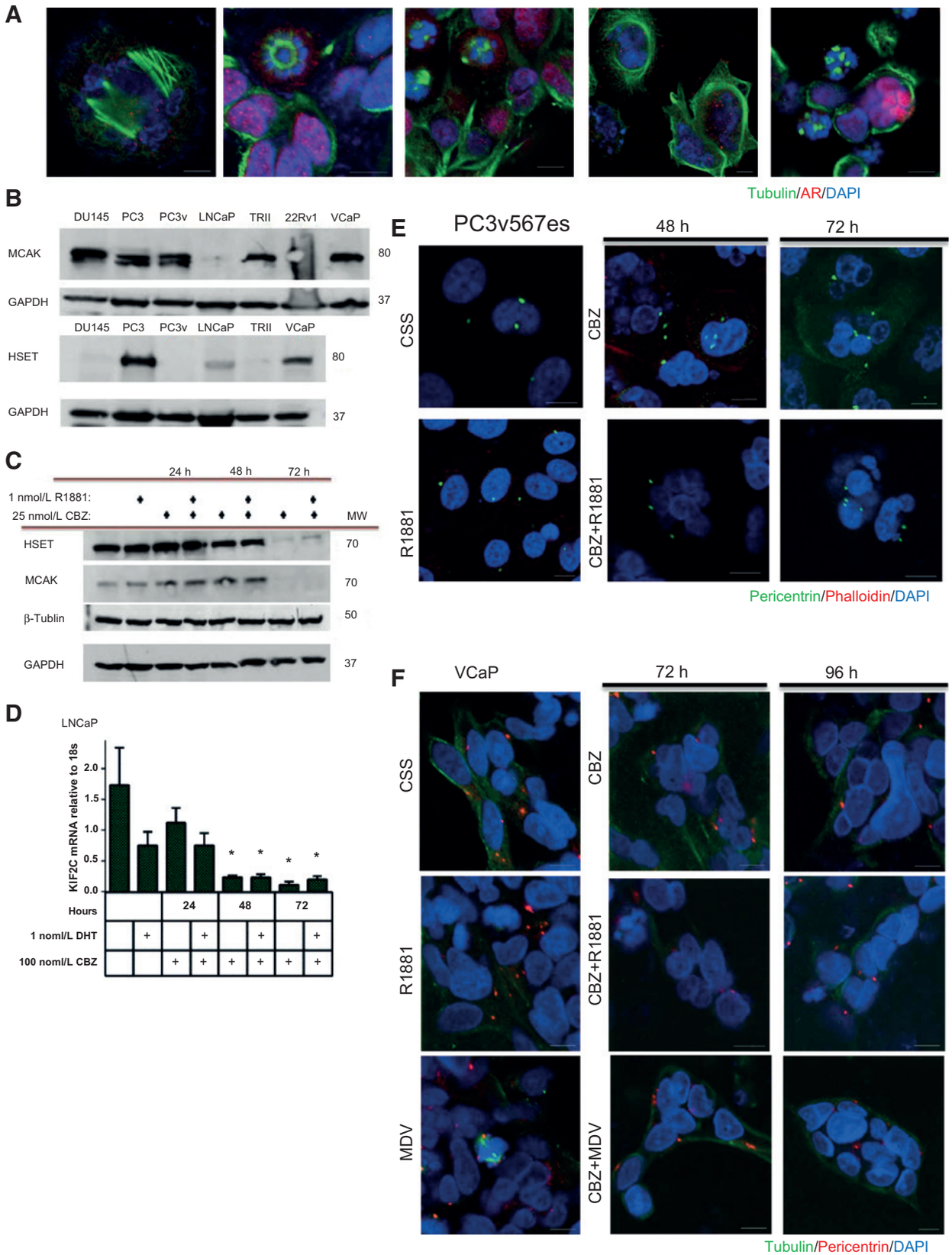

high expression of both proteins (Fig. 3B). DU145 and PC3v567es have high expression of MCAK but completely lack HSET protein expression (Fig. 3B). In response to cabazitaxel (24, 48, or 72 hours) alone or under androgenic pulse, there was a transient increase in expression of MCAK and HSET kinesins within the first 24 hours in the VCaP cells; by 72 hours of treatment, kinesin levels were significantly downregulated (Fig. 3C and Supplementary Fig. S4A). In addition, there was a significant decrease in MCAK (KIF2C) mRNA expression in LNCaP and VCaP cells (Fig. 3D and Supplementary Fig. S4) and in HSET (KIFC1) mRNA levels for VCaP cells (Supplementary Fig. S4B and S4C) in response to cabazitaxel. To determine the potential link between the action of cabazitaxel on mitotic spindle formation and resistance, we subsequently examined pericentrin (marker of centrosomes) expression in the cabazitaxel-resistant prostate cancer PCv567es and VCaP cells and the cabazitaxel-sensitive CRPC 22Rv1 cells. As shown in Fig. 3E, in response to cabazitaxel, PC3v567es and VCaP cells exhibited centrosome clustering and amplification accompanied with severe multinucleation; these effects were not influenced by the status of androgen axis (presence of androgens or antiandrogen, MDV; Fig. 3F). In the CRPC 22Rv1 cells, cabazitaxel treatment led to multinucleation but not centrosomal amplification (Supplementary Fig. S5A).

In vivo novel action of cabazitaxel in models of advanced prostate cancer via induction of MET and glandular differentiation

To define the physiologic significance of our *in vitro* findings, we investigated the antitumor action of cabazitaxel in an *in vivo* model we previously established (TRAMP mice crossed with mice expressing a conditional dominant negative TGFβRII; ref. 35). This TRAMP/DNTGFβRII model is characterized by aggressive tumor progression to metastasis driven by EMT. The consequences of cabazitaxel treatment on the phenotypic landscape and growth dynamics were evaluated in prostate tumors from ($N = 10$) 16 to 18–week-old male mice (castrate vs. non-castrate groups) receiving treatment for 14 days with pharmacologic dose of cabazitaxel (Supplementary Fig. S6A and S6B). Cabazitaxel treatment led to a significant decrease in the body weight as well as the prostate weight ($P < 0.005$; Supplementary Fig. S6C and S6D, respectively; $P < 0.005$). At 18 to 20 weeks, TRAMP+DNTGFBRII+ mice progressed to poorly differentiated prostate cancer (35); histopathologic evaluation (H&E staining) revealed that cabazitaxel alone or in combination with androgen depletion restored the glandular structures and luminal secretions of the prostate epithelium compared with controls (Fig. 4A). Immunoreactivity of cytokeratin-18, a luminal cell and glandular differentiation marker, was markedly increased in tumors from cabazitaxel-treated mice (noncastrate and castrate) compared with VHC (Fig. 4E).

Evaluation of prostate tumor cell–proliferative capacity based on Ki-67 and pH3 immunoreactivity revealed an increased proliferative activity in response to cabazitaxel alone, whereas castration-induced androgen deprivation resulted in a significant decrease in the proliferative index (Fig. 4A and D). To correlate the effect of cabazitaxel on the mitotic spindle with resulting multinucleation (observed *in vitro*; Fig. 3), expression of the nuclear protein pH3 was examined in prostate tumors. As shown in Fig. 4A (bottom), cabazitaxel resulted in distinct multinucleation among prostate tumor glands from cabazitaxel-treated mice, compared with VHC (Fig. 4B, arrows). There was an increased number of TUNEL-positive prostate tumor cells after castration-induced androgen withdrawal, indicating apoptosis induction ($P < 0.005$; Fig. 4A and C). Treatment of either intact or androgen-depleted mice with cabazitaxel (2 weeks) did not induce significant apoptosis (Fig. 4A and C).

The potential contribution of EMT-MET cycling to the glandular formation and reversion to differentiated prostate epithelium by cabazitaxel was subsequently interrogated. Figure 5A indicates representative images of immunoreactivity analysis of the EMT landscape. Certain populations of tumor epithelial cells exhibited strong E-cadherin immunoreactivity paralleled by decreased N-cadherin expression in response to cabazitaxel, supporting an effect on reversing EMT (Fig. 5A). We previously showed that prostate tumors from TRAMP+DNTGFBRII mice exhibit accelerated progression to metastatic disease via changes in the tumor microenvironment driven by increased inflammation and EMT (35). We found that cabazitaxel alone or in combination with androgen depletion reversed EMT to MET as reflected by elevated E-cadherin and decreased N-cadherin immunoreactivity (Fig. 5A). Intense nuclear immunoreactivity for AR was detected in prostate tumors from VHC mice; upon castration-induced ADT, there was a marked reduction in nuclear AR associated with a diffused localization to the cytoplasm (Fig. 5B and C). Treatment of intact mice with cabazitaxel significantly increased nuclear AR, compared with androgen depletion–mediated cytoplasmic translocation (Fig. 5B and C). Prostate tumor epithelial cells in castrate mice treated with cabazitaxel (for 2 weeks) exhibited a reduced AR expression with a significant reduction of nuclear AR compared with controls or cabazitaxel alone treated mice (Fig. 5B and C).

The kinesin immunoreactivity profile in prostate tumors from the transgenic mouse model revealed decreased MCAK expression in response to cabazitaxel (given as a single agent) compared with VHC, castration-androgen depletion, or combination of cabazitaxel with castration (Fig. 5B). Impairing the androgen axis (castration) alone or in combination with cabazitaxel led to increased kinesin expression (Fig. 5B). We

Figure 3.
Cabazitaxel results in multinucleation and centrosome clustering in prostate cancer cells by targeting kinesins. A, left to right, DU145 treated with cabazitaxel (35 nmol/L; 96 hours) exhibit multipolar spindle and microtubule bundling; LNCaP cells treated with cabazitaxel (35 nmol/L; 48 hours) exhibit monoastral spindle formation; LNCaP prostate cancer cells exhibit multipolar spindle after treatment with cabazitaxel (72 hours); PC3 cells overexpressing the AR variant V7 and VCaP cells exhibit extensive multinucleation and multipolar spindle in response to cabazitaxel (100 μmol/L); scale bars, 10 μm. B, expression profile of KIF2C (MCAK) and KIFC1 (HSET) proteins in prostate cancer cells. C, expression of HSET, MCAK, and β-tubulin in LNCaP cells treated with cabazitaxel. GAPDH was used as loading control. D, RT-PCR analysis of mRNA expression of KIF2C in LNCaP cells. E, detection of pericentrin (green), actin (phalloidin-red), and DAPI (blue) in PC3v56es cells after cabazitaxel treatment. F, VCaP cells exhibit multinucleation and centrosome amplification in response to cabazitaxel; scale bars, 10 μm. E, detection of pericentrin (red), tubulin (green), and DAPI (blue) in VCaP cells in response to cabazitaxel and/or MDV (1 μmol/L). 40× oil immersion; scale bars, 10 μm.

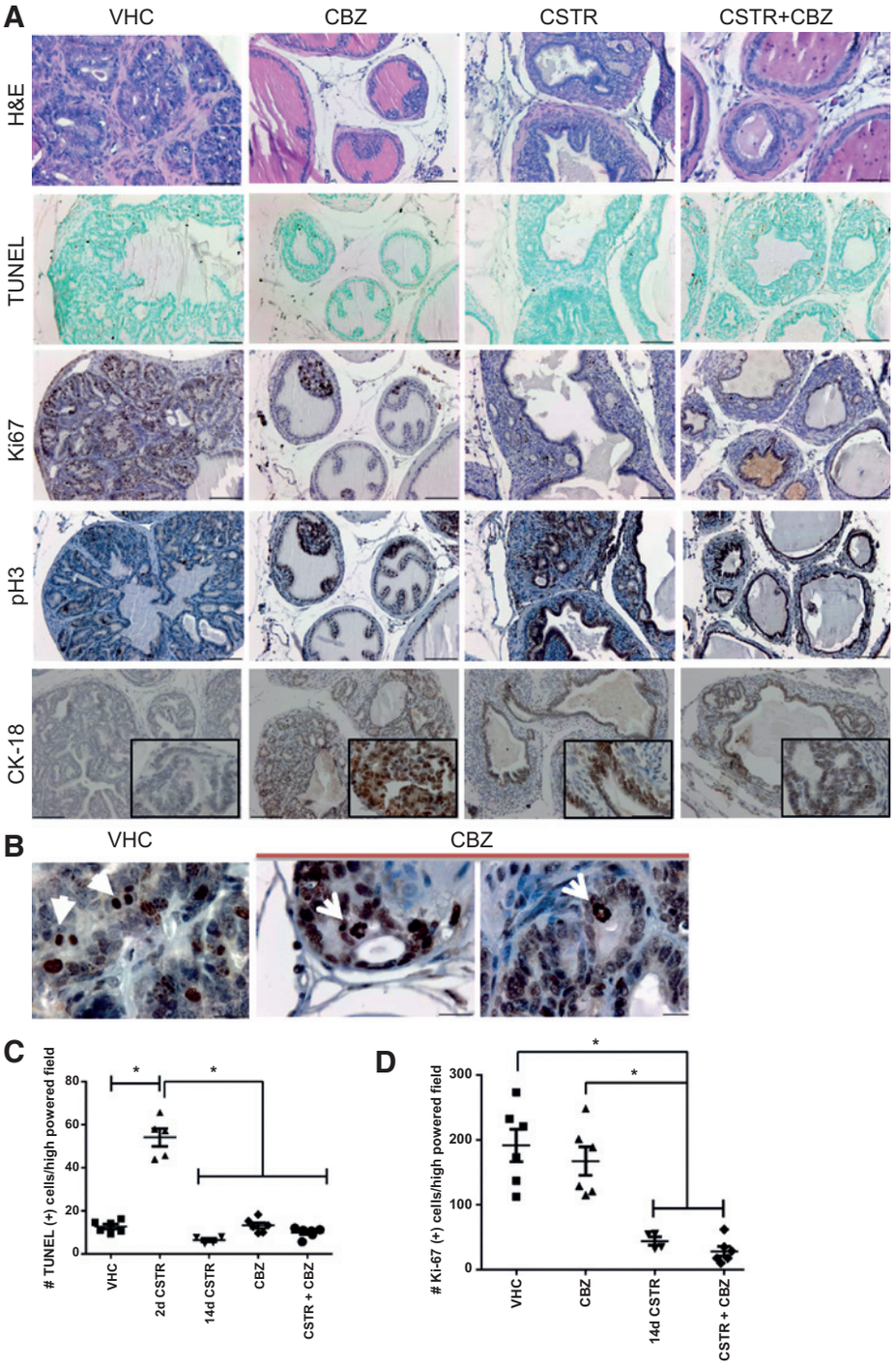

Figure 4.
In vivo effect of cabazitaxel in an androgen-responsive prostate cancer model of progression to lethal disease. A, histopathologic appearance of prostate tumors from transgenic mouse model of prostate tumor progression TRAMP/DNTGFβRII (magnification, ×400; scale bars 50 μm). Serial sections from tumors from control mice (VHC) castrated for 14 days (CSTR) or treated with cabazitaxel for 14 days alone (cabazitaxel) or in combination with castration (CSTR+cabazitaxel) were subjected to apoptosis detection (TUNEL) and cell proliferation (Ki-67 and pH3 nuclear staining). A, bottom, cytokeratin-18 immunoreactivity in tumor sections from VHC, cabazitaxel-treated, castrated, and combination-treated transgenic mice. Prostate tumors (from same littermates) were subjected to immunostaining for CK-18, a marker of luminal glandular differentiation and visualized under ×400 (inset at ×1,000 magnification); scale bars, 50 μm. B, pH3 expression identifying endoreduplication of prostate tumor nuclei after cabazitaxel treatment; magnification, ×100; scale bars 50 μm. C and D, mean number of apoptotic and proliferating prostate tumor cells, respectively, ± SEM; *, $P < 0.05$.

subsequently examined the effect of cabazitaxel on the gene expression profile of EMT regulators in androgen-responsive prostate cancer cell lines, VCaP and LNCaP. RT-PCR analysis of mRNA expression for E-cadherin, vimentin, and Twist1 (Fig. 5D–F respectively) in VCaP cells in response to cabazitaxel demonstrated a significant downregulation in all three genes within 24 hours of treatment that was not affected by DHT. A similar profile of mRNA downregulation for EMT effectors in response to cabazitaxel was observed in LNCaP cells (Fig. 5G–I).

The *in vivo* antitumor effect of cabazitaxel alone or in combination with antiandrogen (MDV) against the human CRPC 22Rv1 xenografts is shown in Fig. 6 (dosing regimen described in Supplementary Fig. S7). Cabazitaxel alone significantly decreased tumor mass in tumor-bearing mice (when compared initiation vs. termination of treatment per individual mouse), although this

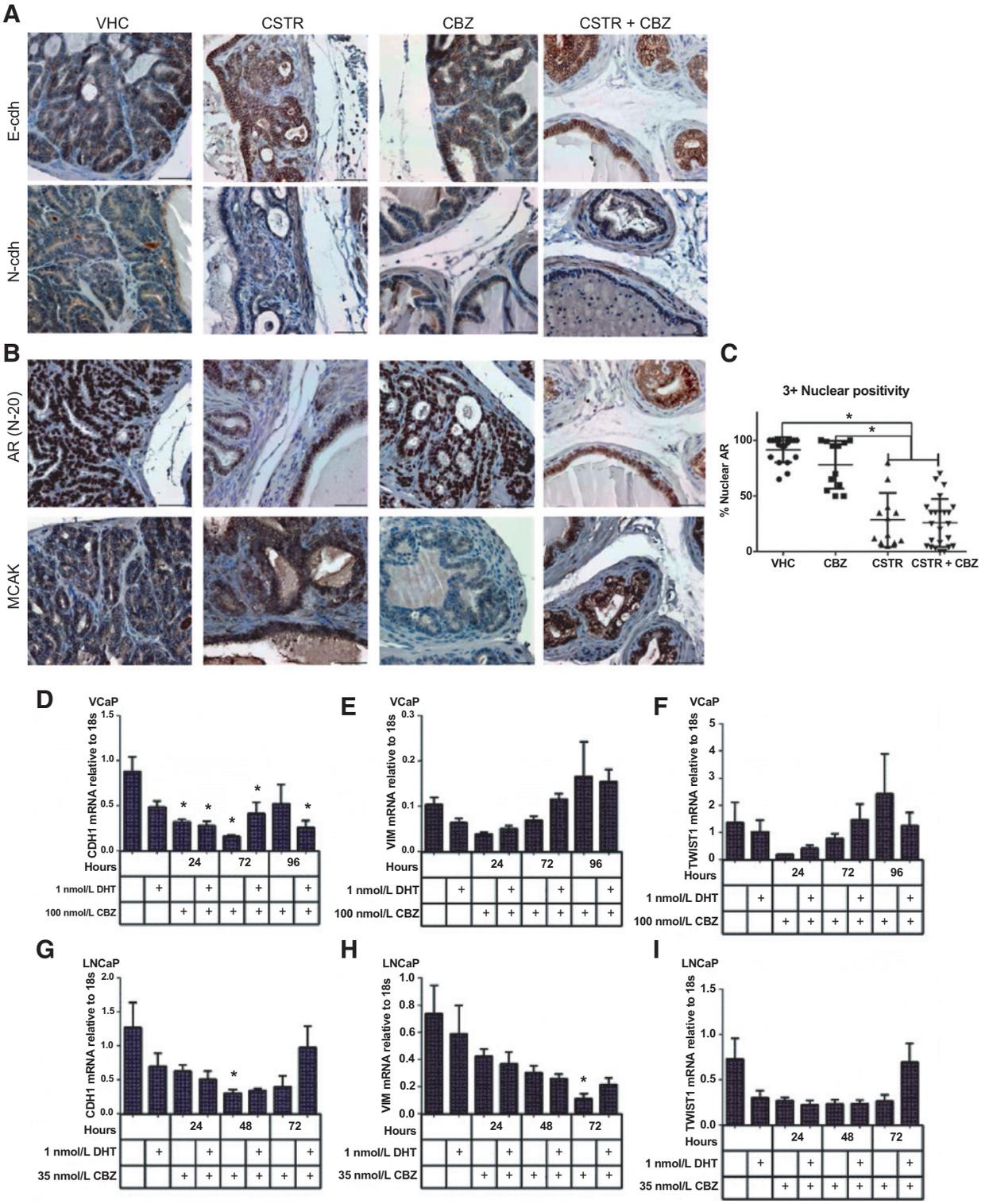

Figure 5.
Cabazitaxel impairs advanced prostate cancer by inducing MET and targeting kinesins. A and B, immunoreactivity profile of E-cadherin (E-cdh), N-cadherin (N-cdh), AR, and MCAK expression in prostate tumor sections from control (VHC), castrated (CSTR), cabazitaxel-treated, or castration and cabazitaxel-treated TRAMP/DNTGFβRII transgenic mice. Cabazitaxel induces EMT changes and reduces AR and kinesin expression. Magnification, ×400; scale bars, 50 μm. C, quantification of AR nuclear staining (3+) in respective sections; mean numerical values (% nuclear AR) ± SEM; *, $P < 0.05$. D–F, RT-PCR analysis of mRNA expression for E-cadherin (CDH1), vimentin (VIM), and Twist1 (TWIST1) in VCaP cells after cabazitaxel treatment. G–I, mRNA profiling of EMT genes in LNCaP cells in response to cabazitaxel. Data represent mean of three independent experiments ± SEM; *, $P < 0.05$ as determined by a two-way ANOVA.

failed to reach statistical significance (Fig. 6A and B). Cabazitaxel alone or in combination with MDV3100 led to a significant reduction in body weight (Supplementary Fig. S7C). Tumor specimens from control (VHC) and treated mice were subjected to immunohistochemical analysis for the tumor growth kinetics, apoptosis and cell proliferation, vascularity, AR, and kinesin expression. Treatment with cabazitaxel alone or in combination with MDV induces significant apoptosis (Fig. 6C and D), whereas the antiandrogen alone failed to induce apoptosis in the CRPC 22Rv1 tumors. Tumor vascularity was inhibited in response to cabazitaxel alone, an effect that was reversed by the combination treatment (Fig. 6C and E). There was a significant increase in Ki-67 immunoreactivity in response to cabazitaxel treatment, but combination with the antiandrogen suppressed prostate tumor proliferation (Fig. 6C and F). Treatment of CRPC 22Rv1 cells with cabazitaxel downregulated MCAK protein in a temporal correlation with the loss of E-cadherin driven by cabazitaxel (Fig. 6G). A pattern of transient changes in AR levels in CRPC 22Rv1 cells was observed in response to cabazitaxel; full-length AR levels were reduced within 24 hours, followed by a significant increase at 48 hours, compared with controls (Fig. 6G).

The impact of cabazitaxel on EMT landscape in the CRPC xenografts was profiled with three marker proteins, E-cadherin, N-cadherin, and ZEB-1. As shown in Fig. 7A, cabazitaxel treatment resulted in increased E-cadherin, while it decreased N-cadherin and ZEB1 immunoreactivity, indicating abrogation of EMT programming in response to the taxane. These *in vivo* phenotypic findings in the CRPC xenograft model are consistent with the effect of the drug in the transgenic model of EMT-driven prostate tumor progression (Fig. 5). Also shown in Fig. 7 is the effect of cabazitaxel on reducing kinesin levels, both MCAK and HSET, in CRPC tumors (Fig. 7B). Antiandrogen treatment had no significant effect on HSET levels, while it reduced MCAK expression. Cabazitaxel treatment reduced AR expression, but it maintained a strong AR nuclear localization in CRPC 22Rv1 tumors compared with MDV3100 or the combination (Fig. 7C).

Discussion

Microtubule-stabilizing chemotherapeutic agents such as docetaxel and paclitaxel have been shown to inhibit AR nuclear localization and activity in human prostate cancer, an action that correlates with the therapeutic response in patients (16, 17). The present results demonstrate that in *in vitro* and *in vivo* models of androgen-sensitive and CRPC-advanced prostate tumors, cabazitaxel chemotherapy maintains AR nuclear localization, while it inhibits AR expression. These observations are in contrast to the effect of docetaxel on preventing nuclear translocation of the AR from the cytosol we and others have reported (16, 17). Moreover, our data demonstrate that the sensitivity of human prostate cancer cells to cabazitaxel was not associated with the AR variant status. Thus, PC3 AR v567es (androgen-independent) and VCaP (androgen-responsive) cells exhibited comparable degree of resistance to cabazitaxel treatment in accord with recent evidence that the antitumor effect of cabazitaxel proceeds via an AR-independent mechanism (38). The mechanisms driving therapeutic cross-resistance to taxanes and antiandrogens in CRPC involve microtubule stabilization and inhibition of AR activity and nuclear localization by interfering with tubulin–AR association (16–18). Compelling evidence identified new signaling effectors conferring mechanistic resistance to taxane chemotherapy in CRPC, including overexpression of ERG genes (39) and activation of the GATA2-IGF2 signaling axis (40).

During cell migration in interphase, centrosome-mediated nucleation of a microtubule array enables directionality, and centrosome amplification promotes transient spindle multipolarity during mitosis and correlates with tumor aggressiveness (41–43). The phenomenon of severe multinucleation that predominated the cabazitaxel-treated prostate cancer cells regardless of AR status, as well as the ability of the drug to induce centrosome amplification promoting spindle multipolarity in the resistant cancer cell lines, provides a shift in our understanding of therapeutic resistance to taxane chemotherapy. This study identified that MCAK is a direct target of cabazitaxel in both androgen-sensitive and CRPC tumors. The kinesin spindle protein (KSP) is a molecular motor that crawls along the microtubules to assist cell division (also known Eg5), and different mitotic kinesins serve specific functions during cell division. In accordance with our findings, MCAK was implicated as a potential mitosis phase target due to its overexpression in CRPC detected in gene expression datasets (44). The effect of cabazitaxel on nuclear AR retention in preclinical models of androgen-sensitive prostate tumors and CRPC is in contrast to docetaxel action (first-line taxane) in promoting cytosolic AR (16, 17). Disruption of the mitotic spindle via direct targeting of mitotic kinesins inducing multinucleation of prostate cancer cells might drive the nuclear retention of AR and inability of microtubules to navigate its cytoplasmic distribution/propagation. As we showed that this effect of cabazitaxel on AR can be overcome by treatment with enzalutamide in androgen-sensitive prostate cancer, the above argument drives a molecular rationale for the therapeutic sequencing of antitumor action of cabazitaxel and the antiandrogen in CRPC tailored to the AR variant status (Fig. 6H).

Cabazitaxel can effectively stabilize microtubule structures in androgen-sensitive and CRPC cells in accordance with the known action of this taxane chemotherapeutic agent (14, 45). With the knowledge that cabazitaxel was designed to bind with β-tubulin subunits and stabilize their interaction preventing depolymerization of the structure, once assembled, the microtubules cannot disassemble, leading to mitotic blockade. In contrast to docetaxel that induced microtubule stabilization leading to classic G_2–M arrest and apoptosis as well as AR cytoplasmic localization, we report for the first time that cabazitaxel treatment induces severe multinucleation and centrosome clustering that led to the development of monoastral spindle formations in the androgen-sensitive prostate cancer cells. Thus, in addition to microtubule stabilization, cabazitaxel targets expression of premitotic kinesins, which facilitate this process (46). The inhibitory effect of cabazitaxel on protein and mRNA expression of MCAK and HSET kinesins provides an initial mechanistic insight into the ability of a microtubule chemotherapy to effectively target a mitotic kinesin and consequently interfering with AR transport across the microtubules, leading to tumor suppression (illustrated on Fig. 6H). Although early-phase clinical trials in CRPC patients using the first-generation Eg5 inhibitor, Ispinesip, have met limited success (45), the concept that kinesins may define therapeutic targeting of cabazitaxel in advanced prostate cancer gains support from evidence documenting a correlation between overexpression of KSP MCAK with CRPC progression and functional involvement of motor protein Eg5 in prostate cancer cell growth (44).

Utilizing a transgenic mouse model of androgen-responsive prostate cancer that is driven by EMT to advanced metastatic

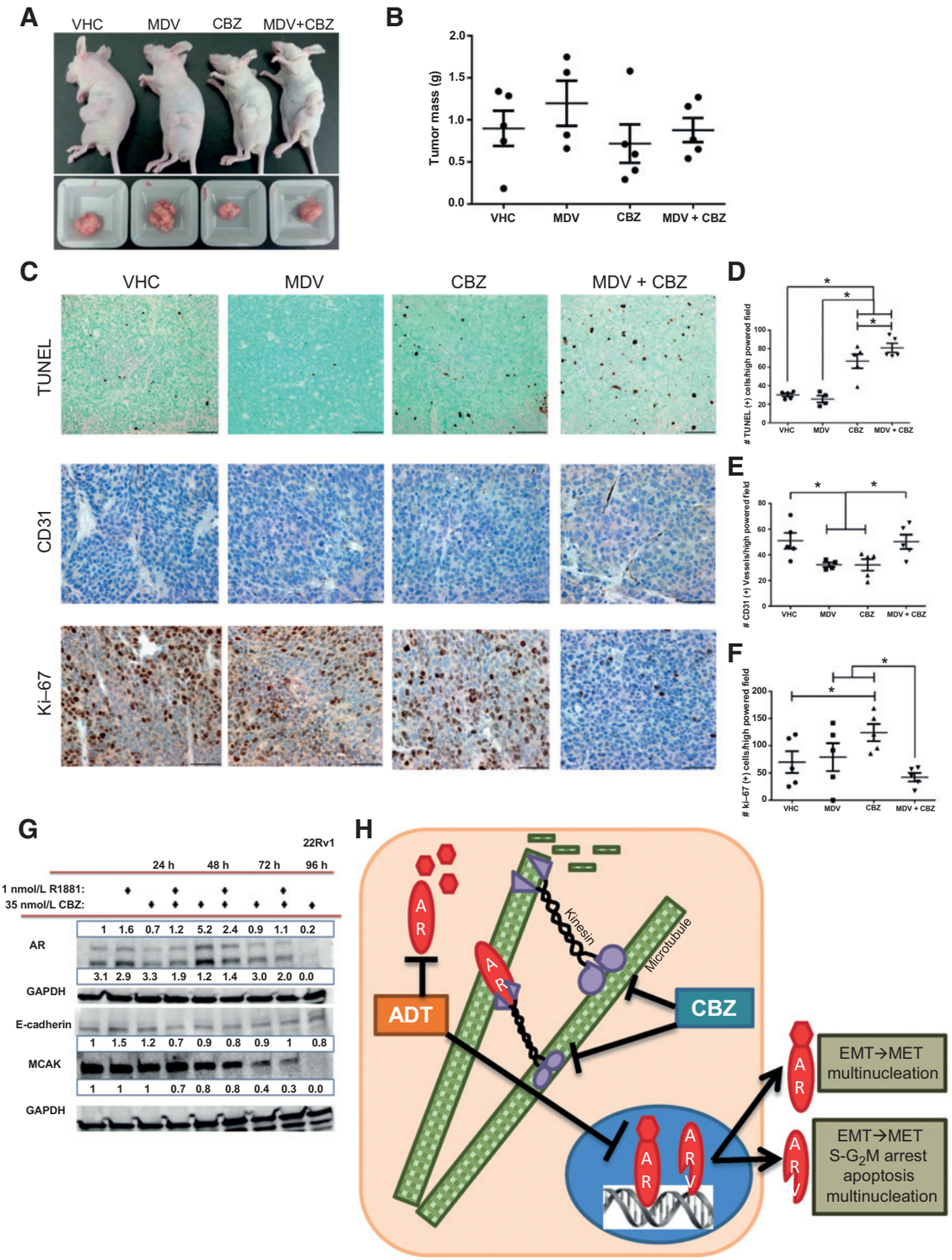

Figure 6.
Effect of cabazitaxel and antiandrogen (enzalutamide) on CRPC xenograft growth. Male nude mice inoculated with CRPC 22Rv1 cells were treated with VHC, cabazitaxel alone, enzalutamide (MDV) or combination (CBZ+MDV) for 2 weeks. A, gross appearance of prostate tumors after various treatments. B, the tumor mass (g) of 22Rv1 CRPC xenografts in response to treatments. C, immunohistochemical assessment of serial sections of 22Rv1 tumors for apoptosis (TUNEL), CD31 (vascularity), and cell proliferation (Ki-67); scale bars, 5 μm. D–F, quantitative analysis of apoptosis, vascularity, and proliferative index (as described in Materials and Methods; mean ± SEM); *, $P < 0.05$. G, protein analysis of AR (N-20), MCAK, and E-cadherin in 22Rv1 cells treated with cabazitaxel. GAPDH, loading control. H, action of cabazitaxel against AR and kinesins causing EMT to MET reversal and multinucleation. The inhibitory effect of cabazitaxel on premitotic kinesins across the microtubules compromises AR nuclear export. Therapeutic response to cabazitaxel proceeds via reversal of EMT to MET and multinucleation.

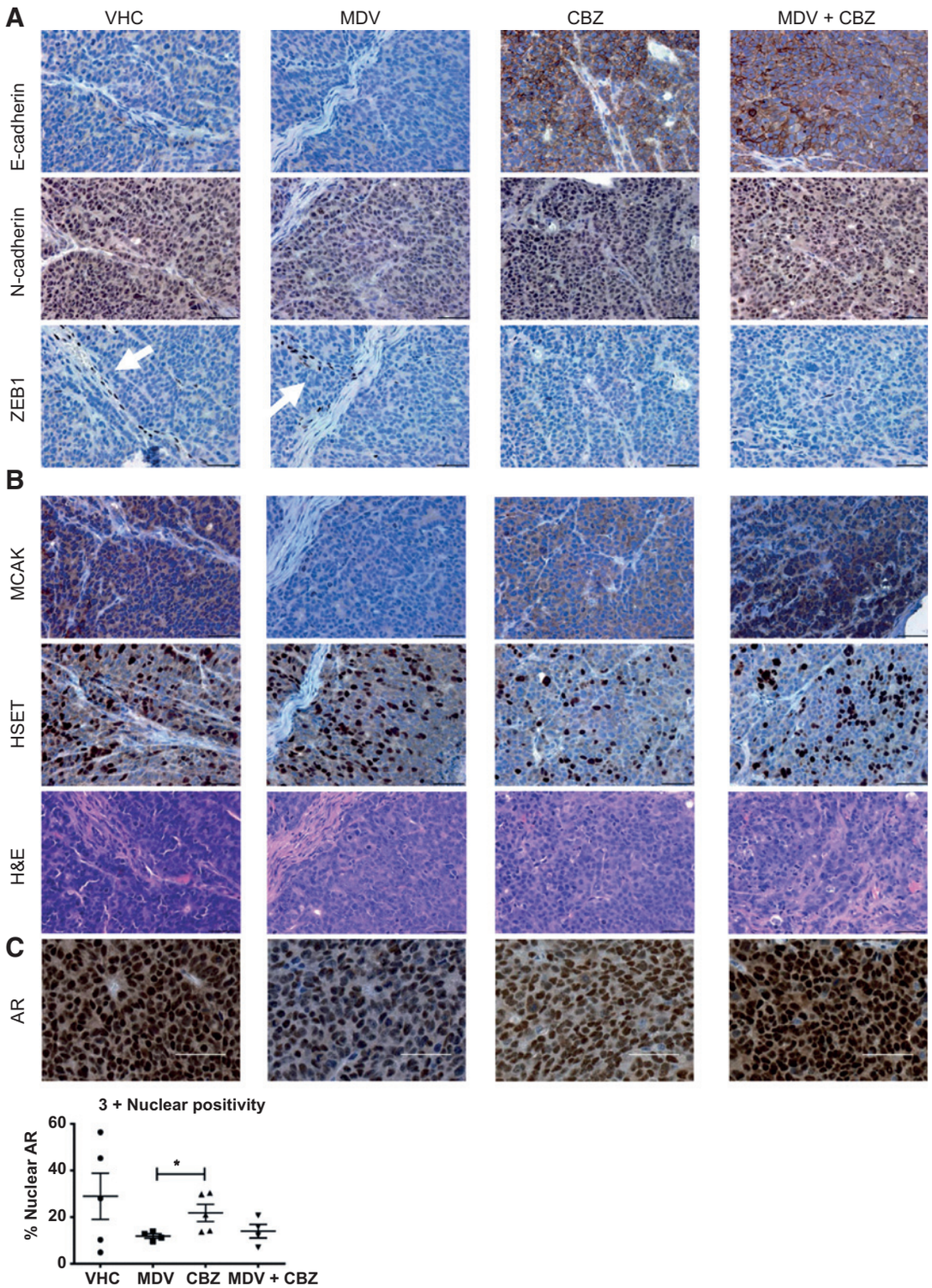

Figure 7.
Impact of cabazitaxel in CRPC via MET, kinesins, and nuclear AR. A, profiling of the EMT landscape in 22Rv1 prostate xenografts in response to cabazitaxel and antiandrogen (MDV) treatment. Serial tumor sections from VHC and treated mice were subjected to immunostaining for E-cadherin, N-cadherin, and Zeb-1; Magnification, ×400; scale bars, 50 μm. B, effect of cabazitaxel on MCAK and HSET protein expression. Bottom, H&E staining of serial sections of CRPC tumors. C, CRPC prostate 22Rv1 tumors from VHC and after treatment with MDV3100, cabazitaxel as single agents or in combination were evaluated for AR. Magnification, ×400. Cabazitaxel reduces AR levels but retains its nuclear localization. Bottom, mean numerical values of cellular distribution of AR (N-20) in prostate tumors ± SEM; *, $P < 0.05$.

disease, we analyzed the consequences of cabazitaxel on EMT in prostate tumor progression *in vivo*. Prostate tumors from mice treated with cabazitaxel alone or in combination with ADT exhibited a phenotypically redifferentiated glandular prostate epithelium with intact luminal secretions. It could be postulated that the plasticity afforded to a fully differentiated epithelium by cabazitaxel allows individual cells to dedifferentiate into mesenchymal-like derivatives in reversible phenotypic transformative process. Thus, several rounds of EMT and MET allow for the formation of well-differentiated glandular epithelial structures in response to cabazitaxel. In a twist of growth kinetics, cabazitaxel increased the proliferative activity of prostate tumor cells. Considering that a dynamic EMT-MET cycling has been functionally implicated in the formation of epithelial tissues (47), our data support the ability of cabazitaxel to induce epithelial differentiation of aggressive prostate tumors via reversal of EMT to MET. Thus, we speculate that upon elimination of the primary population of prostate cancer cells targeted by cabazitaxel, a subset of prostate tumor epithelial cells undergo MET, and this reversion to glandular differentiated epithelial cells primes prostate tumors to the antiandrogen action towards overcoming resistance, highlighting the therapeutic value in the cycling of EMT to MET (Fig. 6H). Moreover, our work provides a molecular basis for the emerging role of AR variants in predicting therapeutic resistance of advanced CRPC to enzalutamide (9) and taxanes in experimental models of CRPC (48). Overexpression of AR splice variants may preclude patients from undergoing cabazitaxel and antiandrogen combination therapy due to therapeutic resistance driven by centrosome clustering. An insight into this cross-resistance is enabled by our observations that the combination of cabazitaxel and enzalutamide leads to a significant growth stimulatory response in the CRPC 22Rv1 cells (harboring AR variants), whereas in the androgen-sensitive VCaP cells, enzalutamide overcame cabazitaxel resistance. Interestingly, it was recently reported that enzalutamide treatment of CRPC 22Rv1 cells had no effect on AR V7 variant expression, whereas it upregulated V7 in VCaP cells (49). Attractive as the biomarker value of AR profiling might emerge in predicting cross-resistance to taxane chemotherapy and antiandrogens in CRPC, one may also consider this new action of cabazitaxel in prostate tumors that bypasses AR and points to an optimized sequencing of these therapeutics, tailored to the EMT landscape.

In summary, this is the first evidence to indicate that cabazitaxel chemotherapy reverses EMT to MET towards phenotypically differentiated prostate glandular/luminal architecture. Cellular redifferentiation via MET conversions may account for the similarities in the phenotypic landscape between primary tumors and bone distant metastatic lesions that can dictate their therapeutic resistance. Ongoing studies investigate (i) the mechanisms driving this remarkable effect of cabazitaxel on tumor glandular differentiation by engaging the microtubule–cytoskeleton interaction and (ii) the consequences of cabazitaxel combination with antiandrogens in clinical prostate tumor specimens from patients with metastatic disease.

Disclosure of Potential Conflicts of Interest

No potential conflicts of interest were disclosed.

Authors' Contributions

Conception and design: S.K. Martin, N. Kyprianou
Development of methodology: S.K. Martin, H. Pu, C. Horbinski, N. Kyprianou
Acquisition of data (provided animals, acquired and managed patients, provided facilities, etc.): S.K. Martin, H. Pu, J.C. Penticuff, Z. Cao, C. Horbinski, N. Kyprianou
Analysis and interpretation of data (e.g., statistical analysis, biostatistics, computational analysis): S.K. Martin, J.C. Penticuff, C. Horbinski, N. Kyprianou
Writing, review, and/or revision of the manuscript: S.K. Martin, Z. Cao, C. Horbinski, N. Kyprianou
Administrative, technical, or material support (i.e., reporting or organizing data, constructing databases): S.K. Martin
Study supervision: N. Kyprianou

Acknowledgments

The authors thank Lorie Howard for her assistance in the submission of the manuscript, Dr. Patrick Hensley for his expert assistance with the preparation of the figures, and Dr. Stephen E. Strup (Department of Urology, University of Kentucky, Lexington, KY) for useful discussions.

Grant Support

This work was supported by funding from Sanofi-Aventis Pharmaceuticals, an NIH/NIDDK R01 DK 083761 grant and the James F. Hardymon Endowment in Urological Research at the University of Kentucky (Lexington, KY).

The costs of publication of this article were defrayed in part by the payment of page charges. This article must therefore be hereby marked *advertisement* in accordance with 18 U.S.C. Section 1734 solely to indicate this fact.

Received July 29, 2015; revised October 20, 2015; accepted October 28, 2015; published OnlineFirst December 8, 2015.

References

1. Huggins C, Hodges CV. Studies on Prostatic Cancer. I. The effect of castration, of estrogen and of androgen injection on serum phosphatase in metastatic carcinoma of the prostate. Cancer Res 1941;1:293–7.
2. Mohler JL. Castration-recurrent prostate cancer is not androgen-independent. Adv Exp Med Biol 2008;617:223–34.
3. Kahn B, Collazo J, Kyprianou N. Androgen receptor as a driver of therapeutic resistance in advanced prostate cancer. Int J Biol Sci 2014;10:588–95.
4. Tran C, Ouk S, Clegg NJ, Chen Y, Watson PA, Arora V, et al. Development of a second generation anti-androgen for treatment of advanced prostate cancer. Science 2009;324:787–90.
5. Ryan CJ, Smith MR, de Bono J, Molina A, Logothetis CJ, de Souza P, et al. Abiraterone in metastatic prostate cancer without previous chemotherapy. N Engl J Med 2013;368:138–48.
6. Beer TM, Armstrong AJ, Rathkopf DE, Loriot Y, Sternberg CN, Higano CS, et al. Enzalutamide in metastatic prostate cancer before chemotherapy. N Engl J Med 2014;371:424–33.
7. Chen CD, Welsbie DS, Tran C, Baek SH, Chen R, Vessella R, et al. Molecular determinants of resistance to antiandrogen therapy. Nat Med 2004;10:33–9.
8. Li Y, Chan SC, Brand LJ, Hwang TH, Silverstein KAT, Dehm SM. Androgen receptor splice variants mediate enzalutamide resistance in castration-resistant prostate cancer cell lines. Cancer Res 2013;73:483–9.
9. Antonarakis ES, Lu C, Wang H, Luber B, Nakazawa M, Roeser JC, et al. AR-V7 and resistance to enzalutamide and abiraterone in prostate cancer. N Engl J Med 2014;371:1028–38.
10. Huizing MT, Misser VHS, Pieters RC, ten Bokkel Huinink WW, Veenhof CHN, Vermorken JB, et al. Taxanes: A new class of antitumor agents. Cancer Invest 1995;13:381–404.

11. Feldman BJ, Feldman D. The development of androgen-independent prostate cancer. Nat Rev 2001;1:34–45.
12. Thadani-Mulero M, Nanus DM, Giannakakou P. Androgen receptor on the move: boarding the microtubule expressway to the nucleus. Cancer Res 2012;72:4611–5.
13. Harrington JA, Jones RJ. Management of metastatic castration-resistant prostate cancer after first-line docetaxel. Eur J Cancer 2011;47:2133–42.
14. Vrignaud P, Semiond D, Lejeune P, Bouchard H, Calvet L, Combeau C, et al. Preclinical antitumor activity of cabazitaxel, a semisynthetic taxane active in taxane-resistant tumors. Clin Cancer Res 2013;19:2973–83.
15. Zhu M, Kyprianou N. Role of androgens and the androgen receptor in epithelial-mesenchymal transition and invasion of prostate cancer cells. FASEB J 2010;24:769–77.
16. Darshan MS, Loftus MS, Thadani-Mulero M, Levy BP, Escuin D, Zhou XK, et al. Taxane-induced blockade to nuclear accumulation of the androgen receptor predicts clinical responses in metastatic prostate cancer. Cancer Res 2011;71:6019–29.
17. Zhu M-L, Horbinski C, Garzotto M, Qian DZ, Beer TM, Kyprianou N. Tubulin-targeting chemotherapy impairs androgen receptor activity in prostate cancer. Cancer Res 2010;70:7992–8002.
18. Mistry SJ, Oh WK. New paradigms in microtubule-mediated endocrine signaling in prostate cancer. Mol Cancer Ther 2013;12:555–66.
19. Gan L, Chen S, Wang Y, Watahiki A, Bohrer L, Sun Z, et al. Inhibition of the androgen receptor as a novel mechanisms of taxol chemotherapy in prostate cancer. Cancer Res 2009;69:8386–94.
20. Fitzpatrick JM, de Wit R. Taxanes mechanisms of action: Potenital implication for treatment sequencing in metastatic castration-resistant prostate cancer. Eur Urol 2014;65:1198–204.
21. Loriot Y, Bianchini D, Ileana E, Sandhu S, Patrikidou A, Pezaro CJ, et al. Antitumour activity of abiraterone acetate against metastatic castration-resistant prostate cancer progressing after docetaxel and enzalutamide (MDV3100). Ann Oncol 2013;00:1–6.
22. Puhr M, Hoefer J, Schafer G, Erb HH, Oh SJ, Klocker H, et al. Epithelial-to-mesenchymal transition leads to docetaxel resistance in prostate cancer and is mediated by reduced expression of miR-200c and miR-205. Am J Pathol 2012;181:2188–201.
23. Pezaro CJ, Omlin AG, Altavilla A, Lorente D, Ferraldeschi R, Bianchini D, et al. Activity of cabazitaxel in castration-resistant prostate cancer progressing after docetaxel and next-generation endocrine agents. Eur Urol 2014;66:459–65.
24. Scher HI, Fizazi K, Saad F, Taplin ME, Sternberg CN, Miller K, et al. Increased survival with enzalutamide in prostate cancer after chemotherapy. N Engl J Med 2012;367:1187–97.
25. Schrader AJ, Boegemann M, Ohlmann C-H, Schnoeller TJ, Krabbe L-M, Hajili T, et al. Enzalutamide in castration-resistant prostate cancer patients after progressing after docetaxel and abiraterone. Eur Urol 2014;65:30–6.
26. Fizazi K, Scher HI, Molina A, Logothetis CJ, Chi K, Jones RJ, et al. Abiraterone acetate for treatment of metastatic castration resistant prostate cancer: final overall survival analysis of the COU-AA-301 randomised, double-blind, placebo-controlled phase 3 study. Lancet Oncol 2012;13:983–92.
27. Korpal M, Korn JM, Gao X, Rakiec DP, Ruddy DA, Doshi S, et al. An F876L mutation in androgen receptor confers genetic and phenotypic resistance to MDV3100 (Enzalutamide). Cancer Discov 2013;3:1030–43.
28. Kalluri R, Weinberg RA. The basics of epithelial-mesenchymal transition. J Clin Invest 2009;119:1420–8.
29. Singh A, Settleman J. EMT, cancer stem cells and drug resistance: an emerging axis of evil in the war on cancer. Oncogene 2010;29:4741–51.
30. Ouyang G, Wang Z, Fang X, Liu J, Yang CJ. Molecular signaling of the epithelial to mesenchymal transition in generating and maintaining cancer stem cells. Cell Mol Life Sci 2010;67:2605–18.
31. Thiery JP, Acloque H, Huang RY, Nieto MA. Epithelial-mesenchymal transitions in development and disease. Cell 2009;139:871–90.
32. Yang J, Weinberg R. Epithelial-mesenchymal transition: at the crossroads of development and tumor metastasis. Dev Cell 2008;14:818–29.
33. Guo Y, Kyprianou N. Restoration of transforming growth factor β signaling pathway in human prostate cancer cells suppresses tumorigenicity via inducation of caspase-1 mediated apoptosis. Cancer Res 1999;59:1366–71.
34. Guo Y, Kyprianou N. Overexpression of transforming growth factor (TGF)β 1 type II receptor restores TGF-β1 sensitivity and signaling in human prostate cancer cells. Cell Growth Differ 1998;9:185–93.
35. Pu H, Collazo J, Jones E, Gayheart D, Sakamoto S, Vogt A, et al. Dysfunctional TGF-Beta Receptor II accelerates prostate cancer tumorigenesis in TRAMP mouse model. Cancer Res 2009;69:7366–74.
36. Martin SK, Banuelos CA, Sadar MD, Kyprianou N. N-terminal targeting of androgen receptor variant enhances response of castration resistant prostate cancer to taxane chemotherapy. Mol Oncol 2015;9:628–39.
37. Rath O, Kozielski F. Kinesins and cancer. Nat Rev Cancer 2012;12:527–39.
38. van Soest RJ, de Morree ES, Kweldam CF, de Ridder CM, Wiemer EA, Mathijssen RH, et al. Targeting the androgen receptor confers in vivo cross-resistance between enzalutamide and docetaxel, but not cabazitaxel, in castration-resistant prostate cancer. Eur Urol 2015;67:981–5.
39. Galletti G, Matov A, Beltran H, Fontugne J, Mosquera JM, Cheung C, et al. ERG induces taxane resistance in castration-resistant prostate cancer. Nat Commun 2014;5:1–12.
40. Vidal SJ, Rodriguez-Bravo V, Quinn SA, Rodriguez-Barrueco R, Lujambio A, Williams E, et al. A targetable GATA2-IGF2 axis confers aggressiveness in lethal prostate cancer. Cancer Cell 2015;27:223–9.
41. Ogden A, Cheng A, Rida PC, Pannu V, Osan R, Clewley R, et al. Quantitative multi-parametric evaluation of centrosome declustering drugs: centrosome amplification, mitotic phenotype, cell cycle and death. Cell Death Dis 2014;5:1–10.
42. Ogden A, Rida PC, Aneja R. Let's huddle to prevent a muddle: centrosome declustering as an attractive anticancer strategy. Cell Death Differ 2012;19:1255–67.
43. Ogden A, Rida PC, Aneja R. Heading off with the herd: how cancer cells might maneuver supernumerary centrosomes for directional migration. Cancer Metastasis Rev 2013;32:269–87.
44. Sircar K, Huang H, Limei H, Liu Y, Dhillon J, Cogdell D, et al. Mitosis phase enrichment with identification of mitotic centromere-associated kinesin as a therapeutic target in castration resistant prostate cancer. PLoS ONE 2012;7:1–8.
45. Azarenko O, Smiyun G, Mah J, Wilson L, Jordan MA. Antiproliferative mechanism of action of the novel taxane cabazitaxel as compared with the parent compound docetaxel in MCF7 breast cancer cells. Mol Cancer Ther 2014;13:2092–103.
46. Nakouzi NA, Le Moulec S, Albiges L, Wang C, Beuzeboc P, Gross-Goupil M, et al. Cabazitaxel remains active in patients progressing after docetaxel followed by novel androgen receptor pathway targeted therapies. Eur Urol 2014;65:.
47. Moreno-Bueno G, Portillo F, Cano A. Transcriptional regulation of cell polarity in EMT and cancer. Oncogene 2008;27:6958–69.
48. Thadani-Mulero M, Portella L, Sun S, Sung M, Matov A, Vessella RL, et al. Androgen receptor splice variants determine taxane sensitivity in prostate cancer. Cancer Res 2014;74:2270–82.
49. Schweizer MT, Antonarakis ES, Wang H, Ajiboye AS, Spitz A, Cao H, et al. Effect of bipolar androgen therapy for asymptomatic men with castration-resistant prostate cancer: results from a pilot clinical study. Sci Transl Med 2015;7:269–72.